Electrical detection of cancer biomarker using aptamers with nanogap break-junctions

2012 Nanotechnology 23 275502

(http://iopscience.iop.org/0957-4484/23/27/275502)

Nanotechnology **23** (2012) 275502 (8pp) doi:10.1088/0957-4484/23/27/275502

Electrical detection of cancer biomarker using aptamers with nanogap break-junctions

Azhar Ilyas[1,2,3], Waseem Asghar[1,2,3], Peter B Allen[4], Holli Duhon[4], Andrew D Ellington[4] and Samir M Iqbal[1,2,3,5,6,7]

[1] Department of Electrical Engineering, University of Texas at Arlington, Arlington, TX 76011, USA
[2] Nanotechnology Research and Education Center, University of Texas at Arlington, Arlington, TX 76019, USA
[3] Nano-Bio Lab, University of Texas at Arlington, Arlington, TX 76019, USA
[4] Institute for Cell and Molecular Biology, University of Texas at Austin, Austin, TX 78712, USA
[5] Joint Graduate Committee of Bioengineering Program, University of Texas at Arlington and University of Texas Southwestern Medical Center at Dallas, Arlington, TX 76010, USA
[6] Department of Bioengineering, University of Texas at Arlington, Arlington, TX 76010, USA

E-mail: smiqbal@uta.edu

Received 26 February 2012, in final form 27 April 2012
Published 18 June 2012
Online at stacks.iop.org/Nano/23/275502

Abstract
Epidermal growth factor receptor (EGFR) is a cell surface protein overexpressed in cancerous cells. It is known to be the most common oncogene. EGFR concentration also increases in the serum of cancer patients. The detection of small changes in the concentration of EGFR can be critical for early diagnosis, resulting in better treatment and improved survival rate of cancer patients. This article reports an RNA aptamer based approach to selectively capture EGFR protein and an electrical scheme for its detection. Pairs of gold electrodes with nanometer separation were made through confluence of focused ion beam scratching and electromigration. The aptamer was hybridized to a single stranded DNA molecule, which in turn was immobilized on the SiO_2 surface between the gold nanoelectrodes. The selectivity of the aptamer was demonstrated by using control chips with mutated non-selective aptamer and with no aptamer. Surface functionalization was characterized by optical detection and two orders of magnitude increase in direct current (DC) was measured when selective capture of EGFR occurred. This represents an electronic biosensor for the detection of proteins of interest for medical applications.

(Some figures may appear in colour only in the online journal)

1. Introduction

The evolution of proteomics has enabled better understanding of disease progression, and helped in establishing new biomarkers for early diagnosis, appropriate treatment and faster drug discovery. Overexpression of epidermal growth factor receptor (EGFR) is considered to be involved in several types of cancer. Its overexpression has been reported as an indication for many cancers like breast, lung, cervical, bladder, esophageal and ovarian cancer [1–6]. The presence of elevated or reduced levels of a biomarker can point out the presence or onset of a disease, specify the phase of that disease and enable monitoring of changes in homeostasis [7]. Elevated levels of EGFR in the serum of lung cancer patients have been reported before. The normal EGFR concentration can be in the range of 45–78 ng ml^{-1}, whereas it may be as much as an order higher in the lymph node metastasis of lung

[7] Address for correspondence: University of Texas at Arlington, 500 South Cooper Street, Room No. 217, Arlington, TX 76019, USA.

cancer patients (850 ng ml^{-1}) [8, 9]. The early detection of a few tens to hundreds of ng ml^{-1} EGFR can be important to improve the prognosis of the patients.

A number of approaches have been reported for the detection of EGFR and its interactions. These techniques incorporate immunohistochemical, flow cytometric, amperometric, mechanical and optical detection modalities [10–15]. Optical waveguides have also been used for label-free sensing to study cell biology and for biomolecular detection [16–19]. These methods of detecting proteins are generally categorized as labeled detection and label-free detection methods. In the case of labeled detection, the presence of proteins is confirmed by some secondary molecule (organic, inorganic or radioactive) that binds to the proteins. Optical detection utilizes a fluorescent tag attached to the proteins and the change in fluorescent intensity after binding signals the presence of proteins, whereas electrical detection directly interrogates the presence of protein molecules. It entails efficient device fabrication in order to define contact structures with a molecular dimension separation. The charge transport properties of a single molecule have also been studied with such structures. Such works have been primarily to identify molecules that may be used as functional electronics components [20–22]. It was recently reported that a single molecule was captured by a probing aptamer between nanogapped single-walled carbon nanotubes (SWCNTs) and charge transport properties were characterized [23].

There have been reports of many types of metal–molecule–metal structure to measure the electrical behavior of molecules [22]. Such structures can be broadly classified as vertical device structures (VDS) and lateral device structures (LDS). VDS utilize a self-assembled monolayer of molecules grown on a metal surface which acts as one contact. The second contact is made through conductive probes of atomic force microscopes, scanning tunneling microscopes or crosswire arrangements [24–26]. An LDS involves a pair of metal contacts with nanometer-sized separation and probes selective to protein molecules are immobilized between the contact structures. Devices of this kind that contain a thin metal strip, in which a gap is created by some technique, are known as break-junctions. Such gaps can be formed through e-beam lithography, electrodeposition of metals or electromigration induced 'breaking' of metal lines [27–31]. These techniques are either slow and costly, mainly because of e-beam writing of the whole structures/lines, or have very low yield of functional devices. This article reports electrical detection of EGFR molecules by making use of a new class of break-junction where a focused ion beam (FIB) is used to scratch a thin metal strip (made with optical lithography and lift-off), followed by conventional microscale probing and electromigration induced breaking to produce break-junctions with high throughput, greater yield, low cost and at an exact spot, as recently reported [32].

Antibodies are mostly used to functionalize surfaces for protein binding and detection. Antibody based devices are not well suited for field-deployable or point-of-care modalities because they require specific ranges of temperature, humidity and ionic strength of the buffer solution in order to retain their function [33]. Low ionic strength is necessary to prevail over surface Debye screening but it causes poor interaction between the target and the surface probes [33]. Recent works have shown significant advancements in introducing aptamers for several types of target molecule [34–41]. Aptamers are reported to be as selective and sensitive as antibodies but exceedingly stable over changing temperature, humidity and ionic concentration [42].

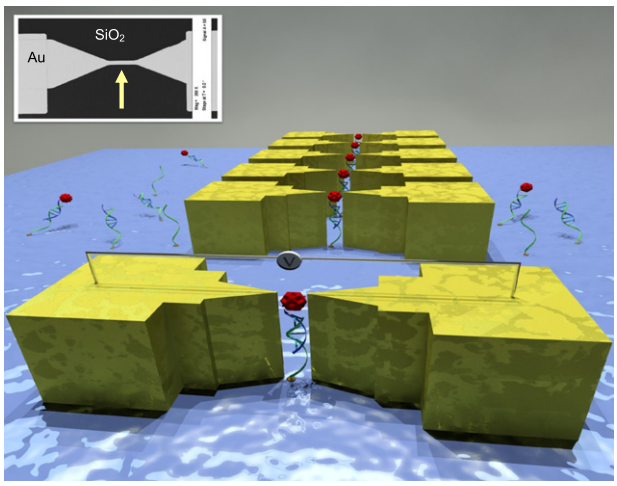

Figure 1. A 3D sketch of the device that demonstrates the mechanism of the electronic detection (not to scale). The inset shows an SEM micrograph of the thin Au line on the SiO_2 chip. Arrow in the inset shows where the scratch is made with FIB.

This article reports cheap and rapid nanoelectrode manufacture and direct current detection of a low concentration of EGFR (50 μg ml^{-1}) binding to RNA aptamers. The effective attachment of RNA aptamers to a chemically modified silicon dioxide surface and EGFR binding to the aptamers was detected with direct current electronic measurements. Figure 1 shows a sketch of the sensor that describes the mechanism of the transduction. The inset shows a scanning electron microscope (SEM) micrograph of the actual device layout. Attachment of the RNA aptamer to the SiO_2 surface and RNA–protein complex interactions were verified with optical measurements as well.

2. Materials and methods

2.1. Materials

The chemicals used for this work were 3′-aminopropyltrieth-oxysilane (APTES); 1,4-phenylene diisothiocyanate (PDITC); ethanol; isopropyl alcohol (IPA); acetone; dimethyl sulfoxide (DMSO); pyridine; 6-amino-1-hexanol; *N*, *N*-dimethylform-amide (DMF); *N*, *N*-diisopropylethylamine (DIPEA); phos-phate buffered saline (PBS); magnesium chloride; hybridiza-tion buffer solution and diethylpyrocarbonate (DEPC) treated de-ionized (DI) water. The chemicals were obtained from Sigma-Aldrich (St Louis, MO, USA). The 5′-amine modified single-strand DNA (ssDNA) was purchased from Alpha DNA (Montreal, Quebec, Canada).

The target molecule was recombinant human EGFR/ErbB1 Fc Chimera (R&D Systems, Minneapolis, MN). The receptor, as per the supplier, was able to bind recombinant human EGF in a functional ELISA at $K_d < 8$ nM.

2.2. Methods

The reported work included three distinct aims that were accomplished towards the final goal of a device to detect EGFR in real-time. The first part involved the fabrication of nanogap break-junctions. The second one elucidated the immobilization of selective probes (aptamers) on the SiO_2 substrates. The third and most important part demonstrates the integration of protein binding and its optical and electrical detection.

2.2.1. Controlled fabrication of nanogap break-junctions. A two-step photolithography process was carried out to define metallic structures on SiO_2 chips. The first layer of pattern was used to create 3 μm wide lines of titanium/gold (thickness 50 Å/150 Å) using metal lift-off. The second step of photolithography defined 200 × 200 μm^2 probing pads that were made of Ti/Au (thickness 100 Å/500 Å) and aligned to the far edges of the lines made in the first lithography/metallization/lift-off. The inset to figure 1 shows the device at this step. The metal lines were partially scratched by an FIB milling process (at the spot highlighted with an arrow in the inset to figure 1). These scratched parts were where the nanogap break-junctions were ultimately made. FIB scratching with gallium ions was carried out at 30 kV acceleration voltage, 1 pA milling current and 2 s per micron scan rate of the beam to achieve the optimum scratch depth. The current–voltage (I–V) characteristics across the metal lines were determined using an Agilent 4155C semiconductor parameter analyzer on a probe station. The I–V measurements before and after the nanomanufacture of the metallic break-junctions were recorded to demonstrate the electromigration effect. The essential advantages of FIB scratching followed by electromigration are to increase the yield of useful devices with the desired gap between electrodes, make the nanogap breaks at precise locations on the line, and narrow the distribution of nanogap sizes. These are not possible with approaches involving only electromigration [21, 43–45].

2.2.2. Aptamer preparation. The aptamer was isolated with a well-known process called 'systematic evolution of ligands by exponential enrichment' (SELEX) as reported before [46, 47]. An iterative selection of binding species against purified human EGFR (R&D Systems, Minneapolis, MN) was carried out to isolate anti-EGFR RNA aptamer [48, 49]. The high affinity ($K_d = 2.4$ nM) anti-EGFR RNA aptamer and a non-functional mutated aptamer were extended with a capture sequence. The extended anti-EGFR aptamer (5′-GGC GCU CCG ACC UUA GUC UCU GUG CCG CUA UAA UGC ACG GAU UUA AUC GCC GUA GAA AAG CAU GUC AAA GCC GGA ACC GUG UAG CAC AGC AGA **GAA UUA AAU GCC CGC CAU GAC CAG**-3′), extended mutant aptamer (5′-GGC GCU CCG ACC UUA GUC UCU GUU CCC ACA UCA UGC ACA AGG ACA AUU CUG UGC AUC CAA GGA GGA GUU CUC GGA ACC GUG UAG CAC AGC AGA **GAA UUA AAU GCC CGC CAU GAC CAG**-3′) and amino modified substrate-anchored probe ssDNA (5′-amine-CTG GTC ATG GCG GGC ATT TAA TTC-3′) were used. The capture sequence has been highlighted in bold font. The capture sequence was the modification of isolated anti-EGFR aptamer and the mutant aptamer. This was made by extending the DNA template at its 3′ end and had 24 nucleotides. The extended capture sequence did not disrupt the aptamer structure but was used to immobilize aptamers on the surface through duplex-formation with the surface-bound ssDNA probe molecules.

2.2.3. Immobilization of probe ssDNA and aptamers on the SiO_2 chip surface. A thermally oxidized silicon wafer was diced into 4 × 4 mm^2 small chips. The chips were initially cleaned in oxygen plasma for 15 min using $Ar + O_2$ at 200 W. This also resulted in a hydrophilic SiO_2 surface. The chips were then immediately immersed in a solution of 2% APTES in ethanol for 1 h at room temperature to silanize the surfaces. The chips were then sequentially rinsed with IPA and DI water and dried in nitrogen flow, followed by curing at 115 °C for 30 min. The chips were then submerged in a solution of 1 mM PDITC in DMSO containing 10% pyridine for 5 to 7 h at 45 °C in order to get PDITC homobifunctional linker molecules attached onto the silanized surface. The chips were then washed sequentially with ethanol and DI water and dried in nitrogen flow. A volume of 8 μl of amine modified ssDNA solution (5 μM concentration of ssDNA in DI water with 50% DMSO, 1% pyridine) was placed on each substrate and allowed to incubate in a humidity chamber for 16 to 18 h at 45 °C to attach amino modified ssDNA to PDITC. After ssDNA attachment, each chip was rinsed sequentially with ethanol and DEPC treated DI water and dried with nitrogen. The functionalized surface was then deactivated and unbound reactive groups of PDITC were capped by submerging the chips in a blocking buffer (BB) solution that contained 50 mM 6-amino-1-hexanol with 150 mM DIPEA in DMF for 1 h. The chips were then rinsed with DMF, ethanol and DEPC treated DI water and dried in a nitrogen stream. After that, a volume of 8 μl of anti-EGFR RNA aptamer solution was placed on every substrate for hybridization. The chips were incubated in the buffer solution (100 nM of anti-EGFR aptamer with 5:1 of DI water and hybridization buffer) at 42 °C for 1 h. The chips were then washed thoroughly with DEPC treated DI water and dried with nitrogen gas. The capture extension of the anti-EGFR RNA aptamer hybridized with the surface-bound complementary ssDNA. In one set of controls, the mutant aptamer was hybridized to surface-bound ssDNA on separate chips using an identical protocol. The presence of ssDNA and RNA aptamers immobilized on the SiO_2 surface was determined by fluorescence measurements of Acridine Orange (AO) stain at an excitation wavelength of 460 nm and an emission wavelength of 650 nm using a

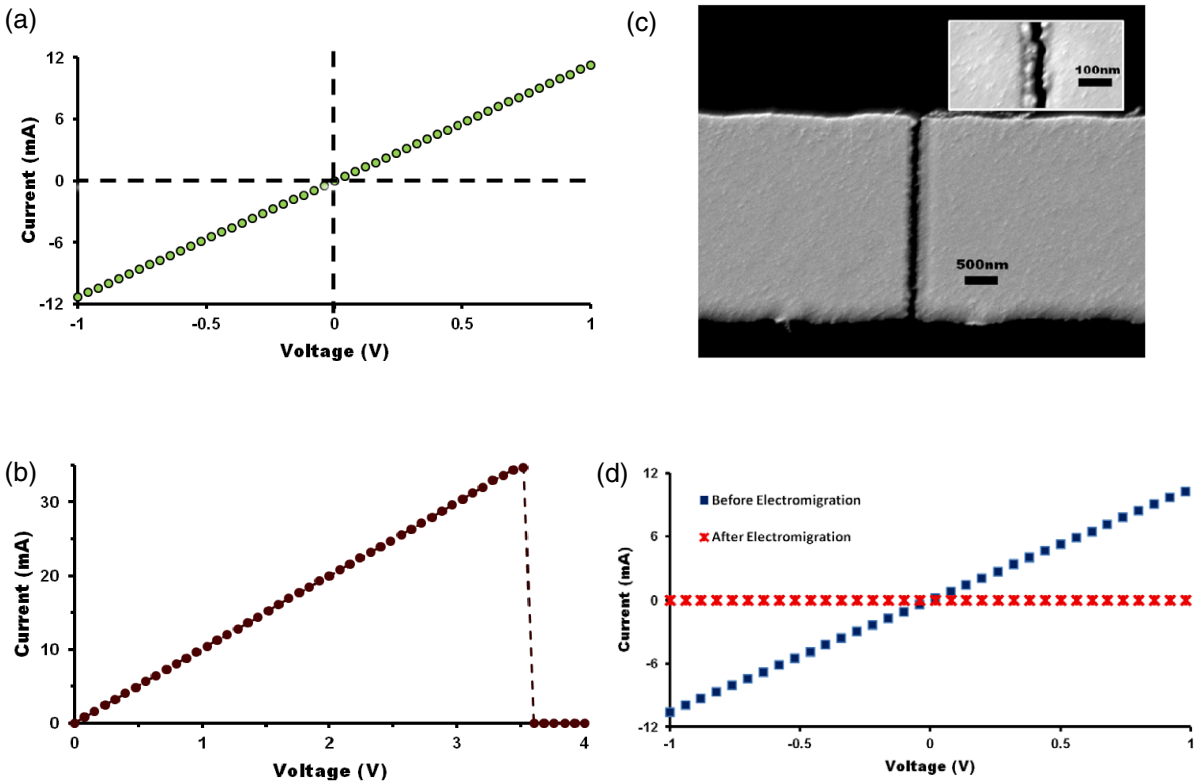

Figure 2. Characterization of the device. (a) Representative *I–V* data after FIB scratching of the metal line show linear Ohmic behavior. (b) A sudden drop in current confirms the complete breaking of the metal line due to electromigration and results in nanogap break-junctions. (c) SEM micrograph showing a clean break between the nanoelectrodes. The inset shows a magnified view of a break-junction with a gap smaller than 30 nm. (d) Comparison of *I–V* data for a representative break-junction before and after the electromigration.

confocal microscope. Another set of controlled chips had no aptamer but underwent all other steps like the aptamer chips.

2.2.4. Protein binding to the probing aptamer. Chips with the attached RNA aptamer were then incubated in 50 ng μl^{-1} of EGFR protein. The solution was prepared in PBS with 5 mM Mg^{2+} and 8 μl of the protein solution was placed on each chip for 45 min at 37 °C. The chips were washed thoroughly with PBS and DEPC treated DI water and dried in the nitrogen flow. The chips were analyzed for the captured EGFR protein by optical detection of fluorescent stain Sypro Ruby Protein Blot at 488 nm wavelength. The fluorescence intensity analysis was done with ImageJ software [50]. Essentially, the surface-bound ssDNA was used to immobilize the anti-EGFR aptamer and subsequently the aptamer was used to capture the EGFR protein.

After confirming the attachment chemistry for RNA immobilization and selectivity of anti-EGFR aptamer on plain chips, electrical detection of EGFR protein was performed using nanomanufactured metallic break-junction devices on oxidized silicon chips. An attachment chemistry exactly identical to that for the plain chips was employed for these devices. Although the concentration of EGFR used was high, the theoretical limit of detection (LOD) of the device is much smaller. As a first order estimate, the protein footstep is about 11 nm and in a nanogap 50 nm long and 3 μm wide, we would need about 400 EGFR copies to fill the whole area of the nanogap [51]. However, the surface charges at the nanoscale, the time of detection, i.e. the time it would take for the EGFR to reach the capture region just by diffusion [52], the steric hindrance and the conformation of molecules are all expected to contribute to the LOD of this framework.

The semiconductor parameter analyzer recorded the direct current tunneling through the nanometer scale electrode separation before and after the protein binding to the probing aptamers in between these nanoelectrodes.

3. Results and discussion

3.1. Fabrication and characterization of the nanometer-sized break-junctions

Optimum FIB scratches were obtained by utilizing our previously reported protocol [32]. The *I–V* data recorded after FIB scratching of the metal lines showed a linear Ohmic behavior that confirmed electrical and physical continuity of the metal lines (figure 2(a)). A voltage sweep from 0 to 4 V broke the metal lines due to electromigration. Figure 2(b) shows a sudden drop in current that depicts an absolute break in the metal line. The SEM micrographs also showed a complete break in the metal lines with nanoscale separation (shown clearly in the inset of figure 2(c)). Figure 2(d) demonstrates a comparison of *I–V* data recorded for the same voltage range (−1 to +1 V) before and after the application of the electromigration-inducing bias. All data and micrographs

of figure 2 are representative for the rest of the devices on the chips.

A very small and random current flow was observed after complete electromigration that showed tunneling current characteristics. The tunneling current in an arrangement of the nanogap electrodes with vacuum as the insulator between them can be approximated as a function of the average barrier height relative to the Fermi level of the negative electrode, the barrier width and the applied voltage across the nanoelectrodes [53].

3.2. Optical detection of immobilized aptamer and captured protein

The surface binding and the presence of ssDNA and RNA aptamer immobilized on the plain SiO_2 chips were confirmed by AO stain and fluorescence measurements. The data of figure 3(a) confirm the binding of ssDNA to the functionalized plain SiO_2 surface while figure 3(b) depicts the hybridization of RNA aptamer to the surface-bound ssDNA. AO stain gives green fluorescence when it interacts with ssDNA whereas a flame-red fluorescence is observed when it interacts with double stranded nucleic acids [54]. The AO stain binds electrostatically to the nucleic acids as it carries positive charge. Electrostatic communication with non-specific polyanions was avoided by using a very low concentration of AO stain (0.2% v/v) and providing a buffer solution with Mg^{2+} and Na^{+} cations that competed with binding to the nucleic acids [55].

EGFR binding to the probing aptamer on the plain chip surface was confirmed with the Sypro Ruby protein gel stain. Sypro Ruby is a ruthenium based stain used to detect the amino acids lysine, arginine and histidine [56]. Figure 3(c) shows a clear enhancement of fluorescent intensity measured from the chips with anti-EGFR aptamer and EGFR protein as compared to that for negative control chips that included probe-functionalized chips not exposed to the target proteins and chips exposed to the target protein but without aptamer immobilized on the surface. The fluorescent intensity was at a maximum when use of a blocking buffer (BB) was omitted and, therefore, unreacted PDITC moieties also contributed towards protein capture. On the other hand, probe-functionalized chips with BB treatment selectively captured the EGFR protein as revealed by a marked increase in fluorescence intensity. The BB was thus used in subsequent experiments to avoid non-specific adsorption/binding on the gold or oxide surfaces.

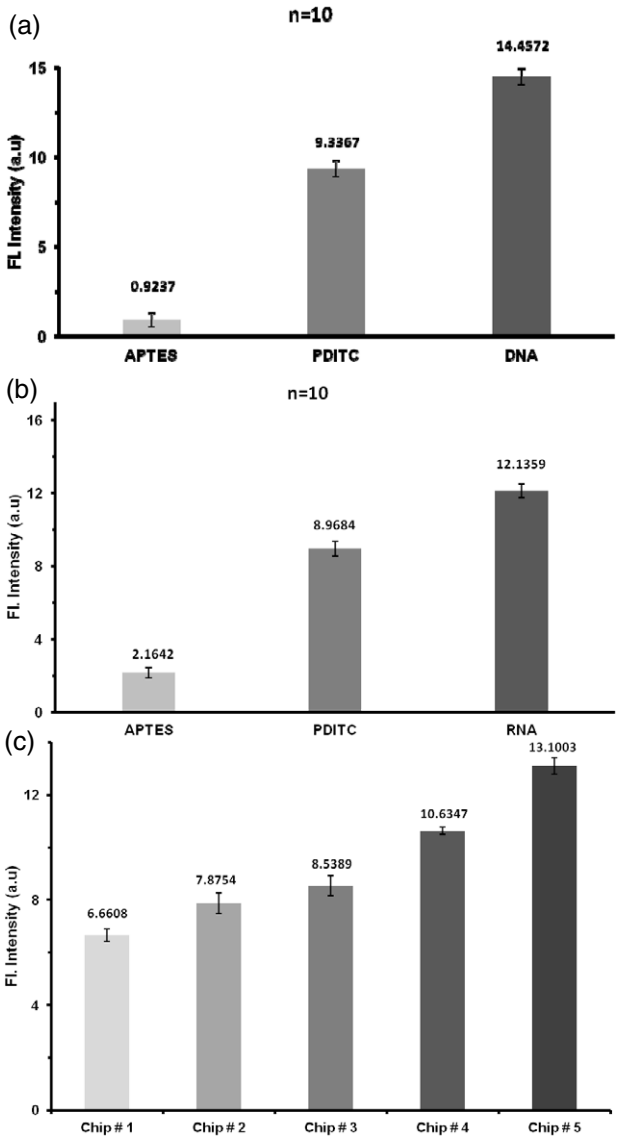

Figure 3. (a) Acridine Orange (AO) stain intensity measurements (background subtracted) depict the presence of surface-bound ssDNA by comparison with control chips ($n = 10$). (b) Fluorescence intensity measurements (background subtracted) using AO confirm the RNA hybridization to surface-bound ssDNA when compared to control chips ($n = 10$). (c) Sypro staining shows the selective capture of EGFR on functionalized SiO_2. From left to right: Chip # 1: control chip treated with blocking buffer (BB) but no aptamer; Chip # 2: control chip with no BB treatment and no aptamer; Chip # 3: control chip functionalized with mutant aptamer and treated with BB; Chip # 4: functionalized chip with anti-EGFR aptamer and captured protein after BB treatment; Chip # 5: functionalized chip with anti-EGFR aptamer and captured protein without using BB. (The error bars represent the standard deviation for $n = 10$.)

3.3. Electrical detection of EGFR binding

Figure 4(a) presents representative data from one device that shows the electronic detection of selective EGFR binding. The control chips with exactly the same devices but with mutant aptamer or no aptamer at all showed no change in conductivity (figure 4(b)). The scrambled sequence of the mutant aptamer prevented it from recognizing the EGFR whereas the anti-EGFR RNA aptamer selectively captured the EGFR. The *I–V* measurements recorded from −1 to +1 V across the metal break-junctions showed a significant increase in current after the capture of EGFR by surface immobilized aptamers. There were two orders of reduction in the resistance through the nanoelectrodes indicating the conducting behavior of the proteins that bridged the nanogap between the electrodes. The yield of devices was 60% which can possibly be increased by tagging the protein molecules with conducting nanoparticles, e.g. of gold. Serum

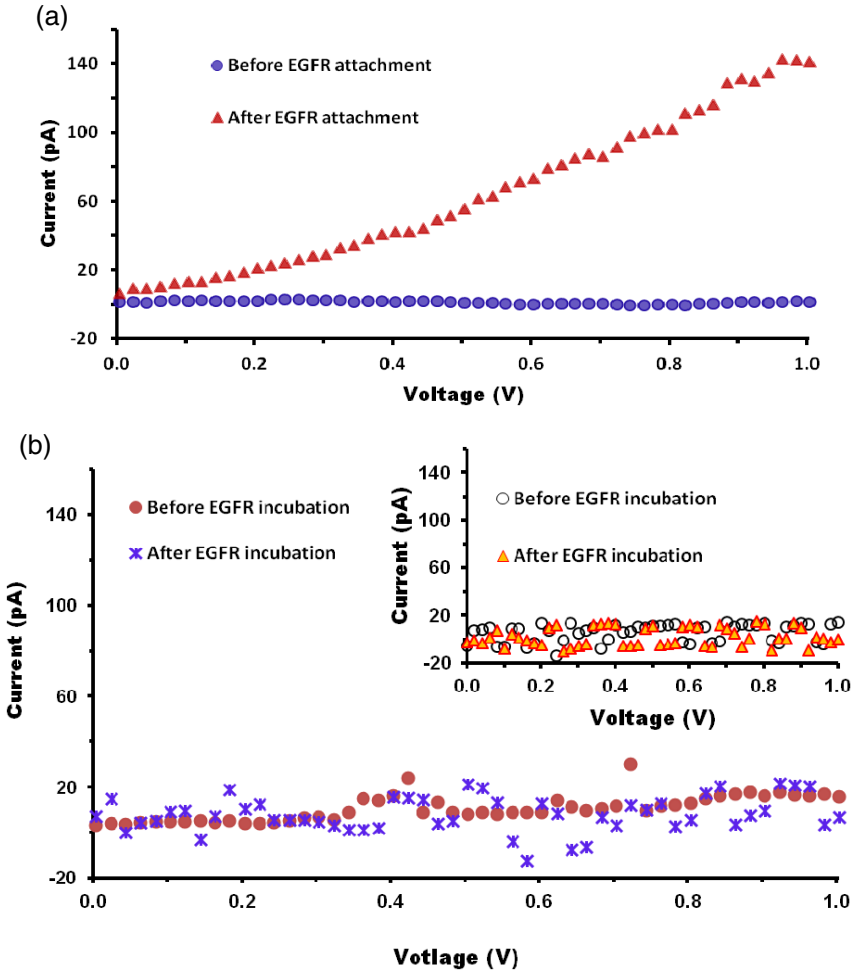

Figure 4. Comparison of *I–V* data for a representative break-junctions before and after exposure to EGFR: (a) the anti-EGFR aptamer chip shows current increase due to the capture of EGFR bridging the nanogap; (b) the mutant aptamer functionalized control chip shows no change in conductivity; the inset shows data for the control chip with no aptamer and thus no change in conductivity. Both controls show no capture of EGFR.

EGFR levels are elevated in many cancers and aptamers isolated through SELEX show high-affinity binding to these. Non-specific binding of the aptamer with non-target serum proteins has already been studied and found to be very atypical [8, 57–59]. Therefore the presented data show the power of this electronic biosensor for direct detection of EGFR present in human serum or plasma.

4. Conclusion

A metallic break-junction framework with precise nanometer-sized separation is presented that utilizes aptamers for selective EGFR capture. The aptamer specifically binds, recognizes and captures EGFR in break-junctions. The capture is electrically detected. The integration of FIB scratching with electromigration provides rapid, cheap and controlled manufacture of nanoscale break-junctions with high yield. The presence of protein between the electrodes shows a robust increase in conductivity between otherwise insulated nanoelectrodes. The detection of a disease linked protein can help in early diagnosis and improved therapy. Such proteonic chips can find applications in many electrical sensors for detection of biologically relevant molecules and species.

Acknowledgments

The authors would like to thank Mohammed A I Mahmood and Syed E A Quadri for their help with the photolithography; F Z Amir for her help with the electron microscopy and Yuan Wan for his guidance with the surface functionalization. This work was supported by National Science Foundation CAREER grant to SMI (ECCS-0845669). Azhar Ilyas and Waseem Asghar were partially supported by a fellowship from the Consortium for Nanomaterials for Aerospace Commerce and Technology (CONTACT) program, Rice University, Houston, TX, USA. Partial chip fabrication was carried out at the Characterization Center for Materials and Biology (C^2MB), and Nanotechnology Research and Education Center, University of Texas at Arlington and Cleanroom Research Laboratory, University of Texas at Dallas. Andrew D Ellington was supported by the Welch

Foundation (grant F-1654) and National Security Science and Engineering Faculty Fellowship (FA9550-10-1-0169). Peter B Allen was supported by NIH Fellowship (F32-GM095280-02).

References

[1] Klijn J G M, Berns P, Schmitz P I M and Foekens J A 1992 The clinical significance of epidermal growth factor receptor (EGF-R) in human breast cancer: a review on 5232 patients *Endocr. Rev.* **13** 3

[2] Lynch T J, Bell D W, Sordella R, Gurubhagavatula S, Okimoto R A, Brannigan B W, Harris P L, Haserlat S M, Supko J G and Haluska F G 2004 Activating mutations in the epidermal growth factor receptor underlying responsiveness of non-small-cell lung cancer to gefitinib *New Engl. J. Med.* **350** 2129

[3] Kersemaekers A M F, Fleuren G J, Kenter G G, Van den Broek L, Uljee S M, Hermans J and Van de Vijver M J 1999 Oncogene alterations in carcinomas of the uterine cervix: overexpression of the epidermal growth factor receptor is associated with poor prognosis *Clin. Cancer Res.* **5** 577

[4] Mellon K, Wright C, Kelly P, Horne C H and Neal D E 1995 Original articles: bladder cancer: long-term outcome related to epidermal growth factor receptor status in bladder cancer *J. Urol.* **153** 919–25

[5] Inada S, Koto T, Futami K, Arima S and Iwashita A 1999 Evaluation of malignancy and the prognosis of esophageal cancer based on an immunohistochemical study (p53, E-cadherin, epidermal growth factor receptor) *Surg. Today* **29** 493–503

[6] Fischer-Colbrie J, Witt A, Heinzl H, Speiser P, Czerwenka K, Sevelda P and Zeillinger R 1997 EGFR and steroid receptors in ovarian carcinoma: comparison with prognostic parameters and outcome of patients *Anticancer Res.* **17** 613–9

[7] Dalton W S and Friend S H 2006 Cancer biomarkers—an invitation to the table *Science* **312** 1165–8

[8] Sasaki H, Yukiue H, Mizuno K, Sekimura A, Konishi A, Yano M, Kaji M, Kiriyama M, Fukai I and Yamakawa Y 2003 Elevated serum epidermal growth factor receptor level is correlated with lymph node metastasis in lung cancer *Int. J. Clin. Oncol.* **8** 79–82

[9] Carney W P, Burrell M, Morris L D and Hamer P J 2002 Normal levels of serum EGFr and decreases in several cancers *Proc. AACR* vol 43

[10] Atkins D, Reiffen K A, Tegtmeier C L, Winther H, Bonato M S and Storkel S 2004 Immunohistochemical detection of EGFR in paraffin-embedded tumor tissues: variation in staining intensity due to choice of fixative and storage time of tissue sections *J. Histochem. Cytochem.* **52** 893

[11] Brockhoff G, Hofstaedter F and Knuechel R 1994 Flow cytometric detection and quantitation of the epidermal growth factor receptor in comparison to Scatchard analysis in human bladder carcinoma cell lines *Cytometry* A **17** 75–83

[12] Lee K W, Hwang K H, Kim C S, Han K, Chung Y B, Park J S, Lee Y M and Moon D C 2001 Determination of recombinant human epidermal growth factor (rhEGF) in a pharmaceutical formulation by high performance liquid chromatography with electrochemical detection *Arch. Pharm. Res.* **24** 355–9

[13] Kippenberger S, Loitsch S, Guschel M, Müller J, Knies Y, Kaufmann R and Bernd A 2005 Mechanical stretch stimulates protein kinase B/Akt phosphorylation in epidermal cells via angiotensin II type 1 receptor and epidermal growth factor receptor *J. Biol. Chem.* **280** 3060

[14] Sako Y, Minoghchi S and Yanagida T 2000 Single-molecule imaging of EGFR signalling on the surface of living cells *Nature Cell Biol.* **2** 168–72

[15] Sorkin A, McClure M, Huang F and Carter R 2000 Interaction of EGF receptor and grb2 in living cells visualized by fluorescence resonance energy transfer (FRET) microscopy *Curr. Biol.* **10** 1395–8

[16] Fang Y and Ferrie A 2007 Optical biosensor differentiates signaling of endogenous PAR1 and PAR2 in A431 cells *BMC Cell Biol.* **8** 24

[17] Ramsden J J and Horvath R 2009 Optical biosensors for cell adhesion *J. Recept. Signal Transduct.* **29** 211–23

[18] Fang Y 2011 Label-free biosensors for cell biology *Int. J. Electrochem.* **2011** 460850

[19] Kozma P, Hamori A, Kurunczi S, Cottier K and Horvath R 2011 Grating coupled optical waveguide interferometer for label-free biosensing *Sensors Actuators* B **155** 446–50

[20] Aviram A and Ratner M A 1974 Molecular rectifiers *Chem. Phys. Lett.* **29** 277–83

[21] Iqbal S M, Balasundaram G, Ghosh S, Bergstrom D E and Bashir R 2005 Direct current electrical characterization of ds-DNA in nanogap junctions *Appl. Phys. Lett.* **86** 153901

[22] Reed M A, Zhou C, Muller C J, Burgin T P and Tour J M 1997 Conductance of a molecular junction *Science* **278** 252

[23] Liu S, Zhang X, Luo W, Wang Z, Guo X, Steigerwald M L and Fang X 2011 Single-molecule detection of proteins using aptamer-functionalized molecular electronic devices *Angew. Chem. Int. Edn* **50** 2496–502

[24] Wold D J and Frisbie C D 2001 Fabrication and characterization of metal–molecule–metal junctions by conducting probe atomic force microscopy *J. Am. Chem. Soc.* **123** 5549–56

[25] Kushmerick J G, Holt D B, Yang J C, Naciri J, Moore M H and Shashidhar R 2002 Metal–molecule contacts and charge transport across monomolecular layers: measurement and theory *Phys. Rev. Lett.* **89** 86802

[26] Datta S, Tian W, Hong S, Reifenberger R, Henderson J I and Kubiak C P 1997 Current–voltage characteristics of self-assembled monolayers by scanning tunneling microscopy *Phys. Rev. Lett.* **79** 2530–3

[27] Liu K, Avouris P, Bucchignano J, Martel R, Sun S and Michl J 2002 Simple fabrication scheme for sub-10 nm electrode gaps using electron-beam lithography *Appl. Phys. Lett.* **80** 865

[28] Zhou C, Muller C J, Deshpande M R, Sleight J W and Reed M A 1995 Microfabrication of a mechanically controllable break junction in silicon *Appl. Phys. Lett.* **67** 1160

[29] Li C Z, He H X and Tao N J 2000 Quantized tunneling current in the metallic nanogaps formed by electrodeposition and etching *Appl. Phys. Lett.* **77** 3995

[30] Park H, Lim A K L, Alivisatos A P, Park J and McEuen P L 1999 Fabrication of metallic electrodes with nanometer separation by electromigration *Appl. Phys. Lett.* **75** 301

[31] Strachan D R, Smith D E, Johnston D E, Park T H, Therien M J, Bonnell D A and Johnson A T 2005 Controlled fabrication of nanogaps in ambient environment for molecular electronics *Appl. Phys. Lett.* **86** 043109

[32] Asghar W, Ramachandran P P, Adewumi A, Noor M R and Iqbal S M 2010 Rapid nanomanufacturing of metallic break junctions using focused ion beam scratching and electromigration *J. Manuf. Sci. Eng.* **132** 030911

[33] Ramachandran P P, Christensen S M and Iqbal S M 2009 Electronic detection of selective proteins using non antibody-based CMOS chip *IEEE NIH Life Science Systems and Applications Workshop (LiSSA'11)* (Bethesda, MD: IEEE) pp 1–4

[34] Song S, Wang L, Li J, Fan C and Zhao J 2008 Aptamer-based biosensors *TRAC Trends Anal. Chem.* **27** 108–17
[35] Zhang H, Wang Z, Li X F and Le X C 2006 Ultrasensitive detection of proteins by amplification of affinity aptamers *Angew. Chem.* **118** 1606–10
[36] Hamaguchi N, Ellington A and Stanton M 2001 Aptamer beacons for the direct detection of proteins *Anal. Biochem.* **294** 126–31
[37] Maehashi K, Katsura T, Kerman K, Takamura Y, Matsumoto K and Tamiya E 2007 Label-free protein biosensor based on aptamer-modified carbon nanotube field-effect transistors *Anal. Chem.* **79** 782–7
[38] Ylera F, Lurz R, Erdmann V A and Fürste J P 2002 Selection of RNA aptamers to the Alzheimer's disease amyloid peptide *Biochem. Biophys. Res. Commun.* **290** 1583–8
[39] Fischer N O, Tarasow T M and Tok J B H 2007 Aptasensors for biosecurity applications *Curr. Opin. Chem. Biol.* **11** 316–28
[40] Zhang H, Wang Z, Li X F and Le X C 2006 Ultrasensitive detection of proteins by amplification of affinity aptamers *Angew. Chem. Int. Edn* **45** 1576–80
[41] Lion N, Rohner T C, Dayon L, Arnaud I L, Damoc E, Youhnovski N, Wu Z Y, Roussel C, Josserand J and Jensen H 1921 Microfluidic systems in proteomics *Electrophoresis* **2003** 3533–62
[42] Bunka D H J and Stockley P G 2006 Aptamers come of age—at last *Nature Rev. Microbiol.* **4** 588–96
[43] Ghosh S, Halimun H, Mahapatro A K, Choi J, Lodha S and Janes D 2005 Device structure for electronic transport through individual molecules using nanoelectrodes *Appl. Phys. Lett.* **87** 233509
[44] Mahapatro A K, Ghosh S and Janes D B 2006 Nanometer scale electrode separation (nanogap) using electromigration at room temperature *IEEE Trans. Nanotechnol.* **5** 232–6
[45] Mahapatro A K, Jeong K J, Lee G U and Janes D B 2007 Sequence specific electronic conduction through polyion-stabilized double-stranded DNA in nanoscale break junctions *Nanotechnology* **18** 195202
[46] Ellington A D and Szostak J W 1990 *In vitro* selection of RNA molecules that bind specific ligands *Nature* **346** 818–22
[47] Stoltenburg R, Reinemann C and Strehlitz B 2007 SELEX—a (r) evolutionary method to generate high-affinity nucleic acid ligands *Biomol. Eng.* **24** 381–403
[48] Li N, Ebright J N, Stovall G M, Chen X, Nguyen H H, Singh A, Syrett A and Ellington A D 2009 Technical and biological issues relevant to cell typing with aptamers *J. Proteome Res.* **8** 2438–48
[49] Li N, Nguyen H H, Byrom M and Ellington A D 2011 Inhibition of cell proliferation by an anti-EGFR aptamer *PLoS One* **6** e20299
[50] NIH ImageJ http://rsbweb.nih.gov/ij (accessed 25 October 2010)
[51] Ilyas A, Asghar W, Billo J A, Syed E A Q and Iqbal S M 2011 From molecular electronics to proteonics: break junctions for biomarker detection *IEEE/NIH Life Science Systems and Applications Workshop (LiSSA'11)* (Bethesda, MD: IEEE) pp 79–82
[52] Nair P R and Alam M A 2006 Performance limits of nanobiosensors *Appl. Phys. Lett.* **88** 233120
[53] Wang W, Lee T and Reed M A 2003 Mechanism of electron conduction in self-assembled alkanethiol monolayer devices *Phys. Rev.* B **68** 35416
[54] McMaster G K and Carmichael G G 1977 Analysis of single-and double-stranded nucleic acids on polyacrylamide and agarose gels by using glyoxal and acridine orange *Proc. Natl Acad. Sci. USA* **74** 4835
[55] Traganos F, Darzynkiewicz Z, Sharpless T and Melamed M R 1977 Simultaneous staining of ribonucleic and deoxyribonucleic acids in unfixed cells using acridine orange in a flow cytofluorometric system *J. Histochem. Cytochem.* **25** 46
[56] Lopez M F, Berggren K, Chernokalskaya E, Lazarev A, Robinson M and Patton W F 2000 A comparison of silver stain and SYPRO Ruby Protein Gel Stain with respect to protein detection in two-dimensional gels and identification by peptide mass profiling *Electrophoresis* **21** 3673–83
[57] Hicke B J and Stephens A W 2000 Escort aptamers: a delivery service for diagnosis and therapy *J. Clin. Invest.* **106** 923–8
[58] Wan Y, Tan J, Asghar W, Kim Y-T, Liu Y and Iqbal S M 2011 Velocity effect on aptamer-based circulating tumor cell isolation in microfluidic devices *J. Phys. Chem.* B **115** 13891–6
[59] Wan Y, Kim Y-T, Li N, Cho S K, Bachoo R, Ellington A D and Iqbal S M 2010 Surface immobilized aptamers for cancer cell isolation and microscopic cytology *Cancer Res.* **70** 11